JOURNAL OF BIOMEDICAL OPTICS 1(1), 83–91 (JANUARY 1996)

COMPUTER-AIDED RETINAL PHOTOCOAGULATION SYSTEM

Steven F. Barrett,[†] Cameron H. G. Wright,[‡] Maya R. Jerath,* R. Stephen Lewis II,[†] Bryan C. Dillard,[†] H. Grady Rylander III,[‡] and Ashley J. Welch[‡]

[†]U. S. Air Force Academy, Department of Electrical Engineering, Colorado 80840; [‡]University of Texas at Austin, Biomedical Engineering Program, ENS 639, Austin, Texas 78712; *Dartmouth College, DHMC, Radiobiology Labs, Lebanon, New Hampshire 03756

(Paper JBO-020 received July 10, 1995; revised manuscript received Oct. 20, 1995; accepted for publication Oct. 31, 1995)

ABSTRACT

Researchers at the University of Texas at Austin's Biomedical Engineering Laser Laboratory and the U. S. Air Force Academy's Department of Electrical Engineering are developing a computer-assisted prototype retinal photocoagulation system. The project goal is to rapidly and precisely automatically place laser lesions in the retina for the treatment of disorders such as diabetic retinopathy and retinal tears while dynamically controlling the extent of the lesion. Separate prototype subsystems have been developed to control lesion parameters (diameter or depth) using lesion reflectance feedback and lesion placement using retinal vessels as tracking landmarks. Successful subsystem testing results *in vivo* on pigmented rabbits using an argon continuous wave laser are presented. A prototype integrated system design to simultaneously control lesion parameters and placement at clinically significant speeds is provided.

Key Words retina; photocoagulation; diabetic retinopathy; automated surgery.

1 INTRODUCTION

Researchers at the University of Texas at Austin and the U. S. Air Force Academy are developing a prototype computer-assisted system to rapidly and precisely place photocoagulation lesions on the retina for the treatment of various retinal disorders such as diabetic retinopathy and retinal tears.[1–4] The project goal is a prototype system that can place lesions of controlled, specified parameters while compensating for patient retinal movement. Early prototype testing results indicate that the lesion depth or diameter can be controlled dynamically and the system can compensate for clinically significant retinal movement.

2 BACKGROUND

Laser photocoagulation of the retina is used to treat various disorders. Two of the most common pathologies are diabetic retinopathy and retinal tears. Diabetic retinopathy, which often occurs in advanced cases of diabetes, is characterized by a hypoxic condition of the retinal tissue. The disease begins in a noninflammatory mode and progresses through increasingly severe stages. The final and most severe stage, the proliferative stage, is characterized by the rapid formation of new, poor-quality blood vessels in a process called neovascularization. These new vessels grow into the vitreous portion of the eye, obstructing the visual path, and may leak blood into the vitreous chamber. This condition is treated with panretinal photocoagulation, in which an all-lines argon laser is used to selectively denature peripheral portions of the retina using laser lesions while sparing the critical vision anatomy about the fovea and optic disk. The retinal vessel network is also spared. While many different lesion patterns may be used, a pattern of two consecutive rings of 200-micron lesions about the critical vision anatomy surrounded by concentric rings of 500-micron lesions out to the far periphery is most common (personal communication, H. G. Rylander III). This treatment protocol may require up to 2000 laser lesions per retina. Panretinal photocoagulation preserves acute vision about the macula at the expense of the peripheral vision. The treatment is based on the hypothesis that the lesions selectively destroy rods and cones by photocoagulation to allow more choroidal oxygen to reach the inner retina. This reduces the need for oxygen from retinal vessels and results in a constriction of these vessels. This selective denaturation improves the oxygen supply to the retina by increasing the oxygen tension, as verified in human patients.[5] The improved oxygen tension suppresses the neovascularization response. The success of argon laser treatment is roughly proportional to the amount of retinal tissue photocoagulated.[6]

Another retinal disorder treated with argon laser lesions is retinal tears or breaks caused by traumatic injuries to the eye, such as a sharp physical blow. The trauma causes the two main layers of the retina

Address all correspondence to Ashley J. Welch. E-mail: welch@aaraya.ece.utexas.edu

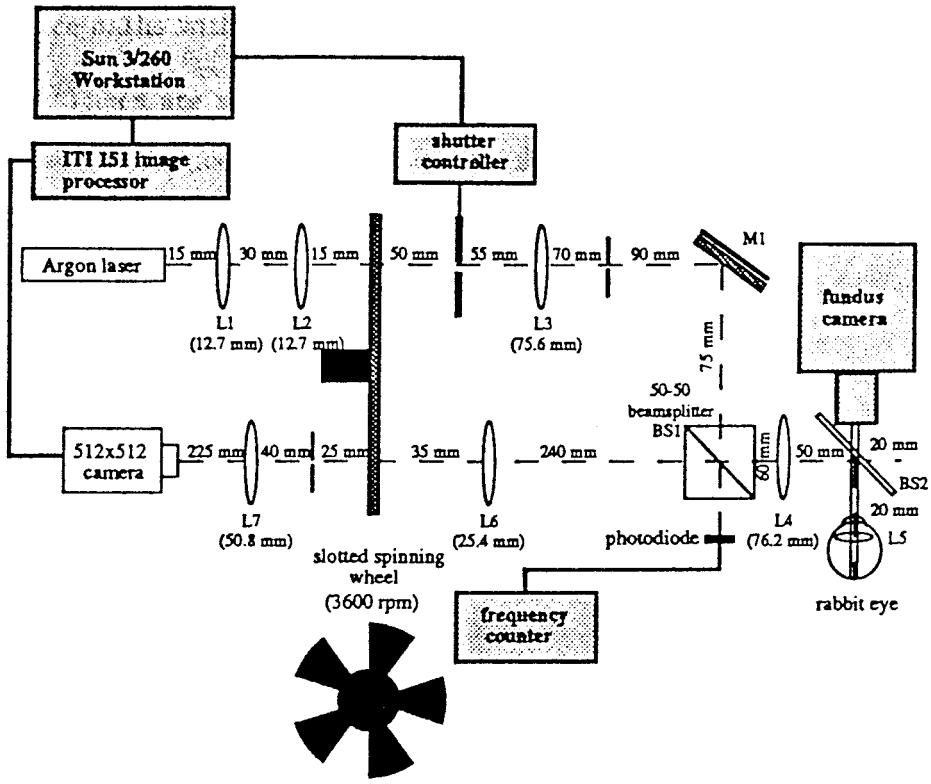

Fig. 1 Lesion depth control subsystem configuration.[9] The system couples the argon laser light and the illumination light of a fundus camera into the eye, and collects the reflectance image with a coaligned CCD video camera.

(the neural retina and the retinal pigment epithelium) to become separated, and the pigment epithelium's nursing role to the rods and cones is disrupted. If the condition is not treated, retinal separation or detachment may result, which can eventually lead to blindness. The retinal breaks and tears may be repaired using photocoagulation to seal the boundary around the break. The rods and cones within the trauma site boundary are no longer functional but deterioration will have been halted.[7] A common technique is to surround the torn area with two continuous, concentric rings of 200 micron lesions.

The size and location of the retinal lesions used to treat retinal disorders is critical for effective results and minimal complications. Currently laser treatment is performed in a ballistic manner. The ophthalmologist aims the laser at each prescribed retinal lesion site and then fires the laser. The laser has a preset power and exposure duration which yields an estimated retinal lesion spot size. Once the laser is fired, no attempt is made to compensate for variability in tissue absorbance, which affects the amount of heat generated, or for retinal movement, which affects lesion placement and size. Furthermore, this procedure is a tedious, tiring task for both the patient and the ophthalmologist.

3 SUBSYSTEM DESCRIPTION

A prototype automated system has been developed for retinal photocoagulation to improve the accuracy and reduce the time required to administer the therapeutic lesions. Separate subsystems have been developed and demonstrated *in vivo* on pigmented rabbits to monitor and control lesion growth dynamically to compensate for tissue inhomogeneity, and to track and compensate for retinal movement during laser irradiation. The results of system development and initial testing have been reported elsewhere.[8–17] A brief review of the two subsystems with testing results is provided here.

3.1 LESION DEPTH CONTROL

The *in vivo* lesion depth control subsystem configuration is provided in Figure 1.[8] A 5-W all-lines argon laser photocoagulator (Coherent System 900) is the source of coagulating light. A standard frame rate monochrome CCD camera (Javelin JE7362) is coaxially aligned with the laser beam. It collects the reflectance signal from the forming lesion. A mydriatic fundus camera (Olympus GRC-W) provides the illumination source for the reflectance image on the retina. To prevent interference between the reflectance signal and the reflected laser light, a chopper wheel is used to alternately shutter the camera and

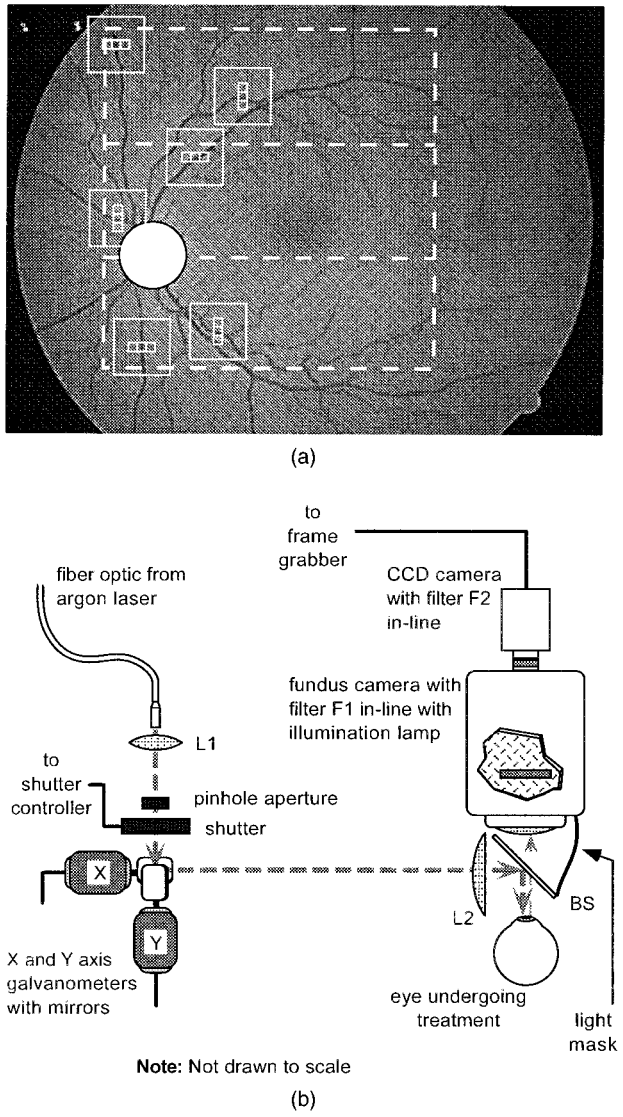

Fig. 2 (a). Six distinct retinal vessel landmarks are referenced together to form a two-dimensional blood vessel template. (b). Lesion placement subsystem. The argon laser light is coaligned with the fundus camera imaging the retinal surface.

laser paths. During photocoagulation, a signal closes the shutter when a preselected central reflectance is measured.

3.2 LESION PLACEMENT

Many researchers have examined the retinal tracking problem.[1–3,18–30] The prototype lesion placement subsystem tracks a specific lesion coordinate on the retinal surface by using blood vessel tracking templates to provide corrective signals to maintain the laser position on the lesion coordinate as shown in Figure 2. Retinal images (512×512) are acquired via a monochrome CCD camera (Panasonic WVCD-20) coupled to a fundus camera and video frame grabber (Matrox PIP-1024). Optical and digital filtering[31,32] is used to enhance the contrast of the retinal vessel network against the lighter retinal background. Details of the tracking software are provided elsewhere.[10,16] Briefly, the frame grabber captures an image of the retina. The template-building algorithm then subdivides a user-specified image region into three separate subregions. The algorithm then exhaustively scans each subregion for the best horizontal and vertical blood vessel templates. The horizontal and vertical templates providing the greatest response are retained as the best template pair from a subregion. This process is repeated on the other two image subregions. The six resulting subtemplates linked in known orientation to one another form a unique two-dimensional tracking template. The desired lesion data base is then built for the treatment of the specific retinal disorder. Algorithms have been developed to automatically build lesion data bases for the treatment of diabetic retinopathy, retinal tears, or a matrix of lesions of user-specified parameters. During the selection of lesion coordinates, the critical anatomy, retinal vessel network, and locations of the tracking templates are masked from possible lesion placement. When the tracking template and lesion data base have been built, retinal tracking may commence. Tracking is accomplished by matching the two-dimensional blood vessel template to the corresponding blood vessel pattern in each video frame. A minimum absolute value of the difference metric is used to determine the template match with the blood vessel features. Once the blood vessel template is located within a video frame, the required location of the laser is calculated since lesion coordinates are known relative to the location of the template's *a priori*. Correction signals are then sent to the X-Y galvanometer pair via the data acquisition and control board to update the laser position. Tracking continues until all lesions specified in the data base have been placed on the retina.

4 SUBSYSTEM *IN VIVO* TESTING

We have tested the lesion depth control subsystem and the laser position subsystem separately *in vivo* on pigmented rabbits to demonstrate the capability of each subsystem separately prior to integrating them into a single prototype system.

4.1 ANIMAL PREPARATION

For the *in vivo* testing, rabbit subjects were handled in accordance with the University of Texas Animal Resource Center protocol T02880906. Humane treatment of the rabbits throughout the experiments was of paramount importance. For each experiment a pigmented crossbred Californian and New Zealand rabbit was anesthetized intramuscularly with a combination of ketamine (ketamine hydrochloride, 35 mg/kg) and Rompun (xylazine hydrochloride, 5.9 mg/kg). Following injection, the rabbit's right pupil was dilated with Mydriacyl 1% (tropicamide 1% ophthalmic solution). Several drops of Alcaine were placed in the eye as a local anesthetic. A

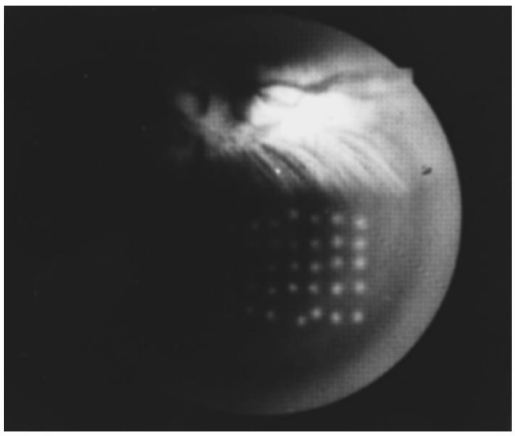

Fig. 3 Small lesion array on rabbit retina (165 mW, 267 ms, 500- micron spot size).

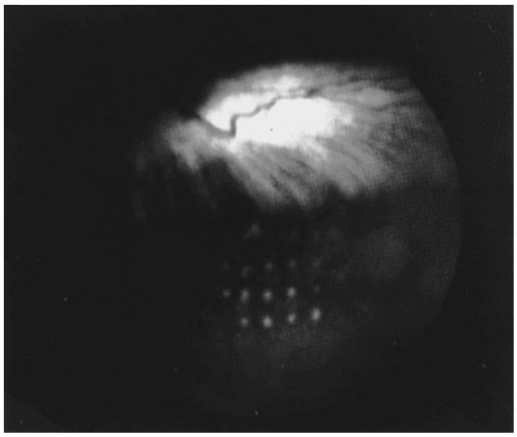

Fig. 4 Small lesion array (55 mW, Row 1: 267 ms, Row 2: 534 ms, Row 3: 801 ms, Row 4: 1068 ms, 500-micron spot size).

speculum (Sontec Instruments 10-1000 Barraquer wire speculum, small) was then inserted to hold the eyelids in an open position. The rabbit was then secured to an animal platform via a safety belt. A 0.9% saline drip was used periodically to irrigate the cornea to maintain moistness. The depth of anesthesia was checked at 5 minute intervals using the toe pinch method. Following the experiment, Ocumycin salve (bacitracin zinc and polymyxin B sulfate ophthalmic ointment) was applied to the eye under the lid. Also, 1 cc of Pen BP-48 (penicillin G benzathine and penicillin G procaine in aqueous suspension) antibiotic was injected intramuscularly.

4.2 LESION DEPTH CONTROL

The lesion depth control subsystem was tested on three different pigmented rabbits and demonstrated the capability to administer feedback-controlled uniform lesions despite variation in tissue absorption or changes in laser parameters.[8,9,11–13]

4.3 LESION PLACEMENT CONTROL

The lesion placement control subsystem was tested on five pigmented rabbits. The capability to constrain an irradiating laser within a 100-micron radius target area for retinal velocities less than 2 degrees per second was demonstrated. Furthermore, the lesion placement subsystem was used to demonstrate the feasibility of placing lesions for the treatment of diabetic retinopathy and retinal tears *in vivo* on pigmented rabbits.[10,14–17] Several *in vivo* experiments were accomplished to demonstrate lesion placement in a rectangular matrix pattern. This matrix pattern is of interest to researchers of laser–tissue interaction studies. Often in these studies laser-induced lesions are not readily visible for subsequent tissue analysis. With this subsystem, laser irradiation sites may be placed in an orderly array so that the sites are precisely known. Lesions were placed in a two-dimensional array with 750-micron spacing between adjacent lesion rows and columns.

In the first matrix experiment, a small matrix pattern was placed on the rabbit retina using a fixed corneal laser power of 165 mW and an exposure time of 267 ms (see Figure 3). For the second matrix experiment, a five-column, four-row matrix pattern was placed using a fixed corneal power of 55 mW. Row 1 had a laser exposure time of 267 ms; Row 2, 534 ms; Row 3, 801 ms; and Row 4, 1068 ms. The purpose of this experiment was to demonstrate the capability of the tracking algorithm to maintain the laser on a specific coordinate during multiple position updates. The resulting laser pattern is illustrated in Figure 4. Results of the initial *in vivo* testing are provided in Table 1.

Since the initial round of *in vivo* testing, an improved lesion placement control subsystem has been tested on a pigmented rabbit. The improved system was hosted on a 486 66-MHz computer as opposed to the 486 33-MHz computer. Laser power was 100 mW at the cornea with a 291-ms exposure time (see Figure 5). Note the improved lesion placement as contrasted with Figures 3 and 4.

The lesion matrix experiments on rabbit subjects demonstrated the capability to rapidly and precisely place lesions on the retina. Only 11.2 s were required to place the lesions in the first small matrix experiment while 13.4 s were required to place the lesions in the second matrix experiment. The prototype system has the capability to constrain the laser beam within a 100-micron radius target area for retinal movements of less than 2 degrees per second. At retinal movements greater than 2 degrees per second but less than 16 degrees per second, the tracking algorithm will maintain a lock on the moving retina but the error radius will be larger. Note in the table that not all attempts resulted in a visible lesion. This is due to variation in retinal absorbance and inability of the present system to strike the far peripheral region of a given retinal field of view. The error provided in the table for each experiment is the worst-case difference between the desired le-

Table 1 Results of initial tests.

Description	Rabbit	Laser parameters: λ (nm), corneal power (mW), spot size (μm), exposure time (ms)	Lesions placed/ lesions attempted	Laydown time (*s*)	Retinal movement (mm^2)	Approximate error (microns)[a)]
Diabetic retinopathy	1888	514 nm, 145 mW, 325 μm, 267.3 ms	33/59	15.7 *s*	1 mm^2	300 μm
Retinal tear	1887	514 nm, 230 mW, 325 μm, 267.3 ms	23/25	6.7 *s*	0.1 mm^2	1,500 μm
Large matrix	1944	514 nm, 155 mW, 460 μm, 267.3 ms	77/86	23.0 *s*	0.48 mm^2	500 μm
Small matrix	1989	514 nm, 165 mW, 420 μm, 267.3 ms	42/42	11.2 *s*	0.16 mm^2	1,000 μm
4 Row× 5 column matrix	1675	514 nm, 55 mW, 325 μm Row 1: 267 ms Row 2: 534 ms Row 3: 801 ms Row 4: 1,068 ms	19/20	13.4 *s*	0.1 mm^2	750 μm

[a] Worst-case error reported, open loop mode, error due primarily to misalignment between retinal observation subsystem and laser pointing subsystem.

sion position and the actual lesion placement. This error is due primarily to having the animal platform on a separate stage from the rest of the subsystem. This error can be minimized by mounting the animal platform on the same stable platform as the lesion placement control subsystem.

5 ONGOING WORK ON AN INTEGRATED SYSTEM: CALOSOS

With successful testing of the lesion depth control subsystem and the lesion placement subsystem accomplished, recent research efforts have concentrated on combining these subsystems into a single prototype system to control simultaneously lesion parameters and placement. This integration project has been designated CALOSOS for computer-aided laser optics system for ophthalmic surgery. Our first CALOSOS prototype, which attempts to combine the capability of both subsystems, is illustrated in Figure 6.

5.1 SYSTEM DESCRIPTION

The CALOSOS project may be subdivided into the system optics, the computer control system used to simultaneously measure lesion depth and control lesion placement, the computer-controlled eye phantom used for system testing, and the data acquisition and recording subsystem. Each of these systems is detailed below.

5.2 OPTICS

The overall objective of the CALOSOS optics system is to precisely place an irradiating argon laser at prescribed lesion coordinates and at prescribed depth parameters on the retina while compensating for any retinal movement by the patient. The optical layout is diagrammed in Figure 7. There are two main optical legs that are coaligned just before the retinal target: (1) the irradiating laser leg and (2) the retinal imaging leg.

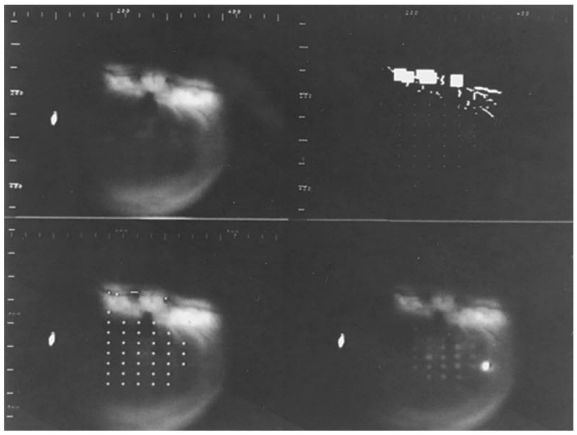

(a)

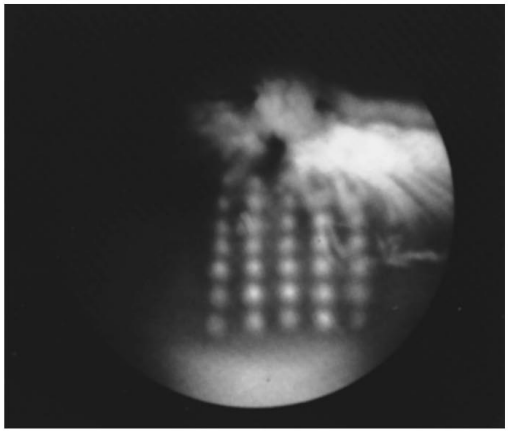

(b)

Fig. 5 *In vivo* testing with an improved lesion placement subsystem. (a): Rabbit retina prior to irradiation. (b): The retinal vessel streak and location of the tracking templates have been masked from lesion placement. The desired locations of the lesion coordinates are plotted prior to irradiation. (c): The locations of the tracking templates along with desired lesion locations have been superimposed upon the target retina. (d): Irradiated lesions immediately post-op (100 mW, 291 ms, 500- micron spot size). (e): Closeup of final result.

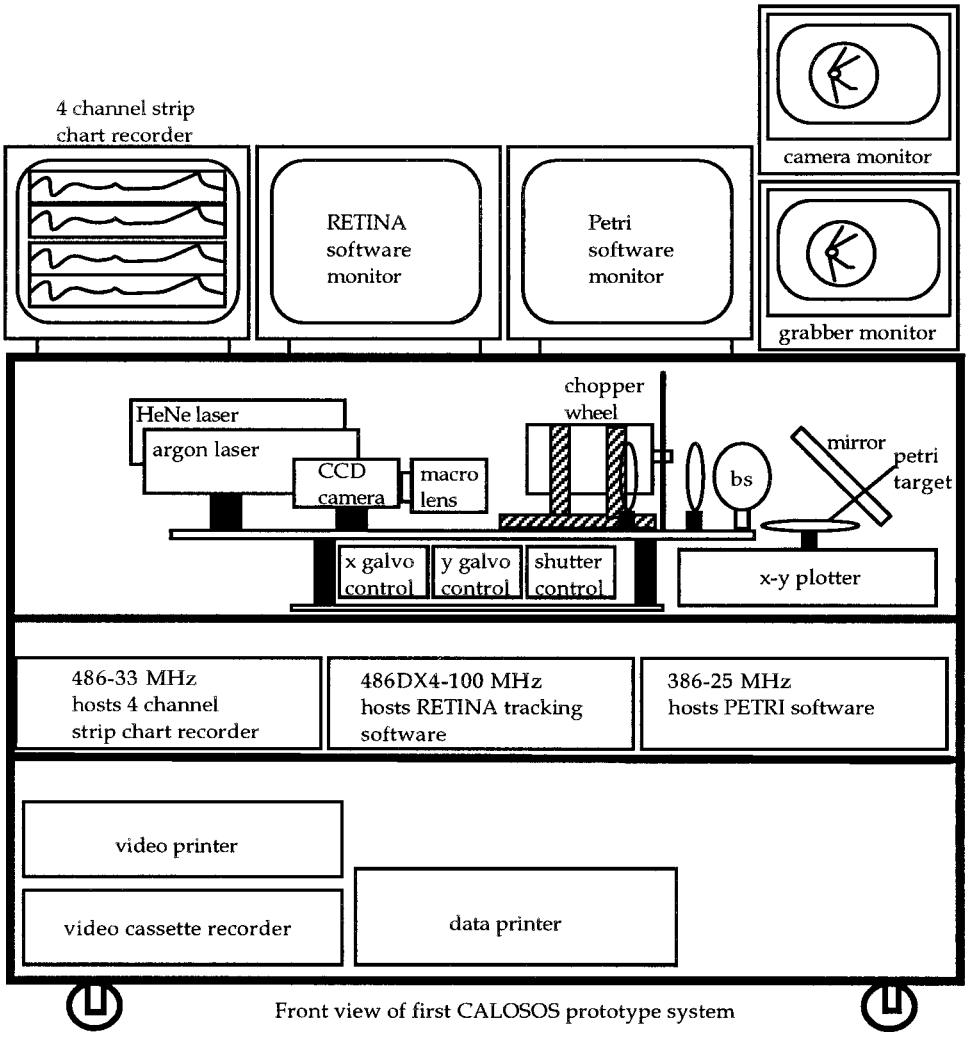

Fig. 6 CALOSOS Prototype.

The irradiating laser leg consists of a line-selectable argon laser and a low-power HeNe alignment laser. The argon laser is used to place the therapeutic lesions on the retina while the HeNe laser is used for system alignment. The argon laser is passed through an aperture to select a homogeneous portion of the beam and then through an electronically controlled shutter with an open time of 1.8 ms and a closed time of 0.8 ms (Uniblitz LS6Z2). In the integrated system, the time the shutter is open will be determined by information derived from the reflectance feedback parameters visible lesion. The argon laser then passes through the blades of a rotating chopper wheel. The two lasers are then coaligned using a system of mirrors and a beam splitter as illustrated in Figure 7. The coaligned beams are then directed to a pair of X-Y galvanometer-controlled mirrors (General Scanning G124). The galvanometers are driven by a pair of scanner drivers (General Scanning AX-200) that are under the control of the system computer. The coaligned beam is steered by the galvanometer pair toward and reflected off of a 50/50 beam splitter that directs the beam to the retinal phantom target.

The retinal imaging leg consists of a standard frame rate monochrome CCD camera with a resolution of 768×494 pixels equipped with a macro lens (Javelin JL35X). The retinal imaging leg is coaligned with the irradiating laser leg via the 50/50 beam splitter. A chopper wheel is used to alternate between the irradiating laser leg and the retinal imaging leg. The chopper wheel prevents the intense irradiating laser from washing out the retinal image captured by the CCD camera by alternately shuttering each optical leg. The chopper wheel rotates at 30 revolutions per second. The five slots in the chopper wheel provide an effective shutter speed of 150 slots per second (a harmonic frequency for a 30 fps CCD array) to prevent camera image beating. An electronic control mechanism was designed to stabilize the chopper wheel motor speed (24 VDC, 1500 rpm motor with optical tachometer, Brother DC-58-108). A pair of biconvex lenses (f=50 mm) is used to demagnify the image as

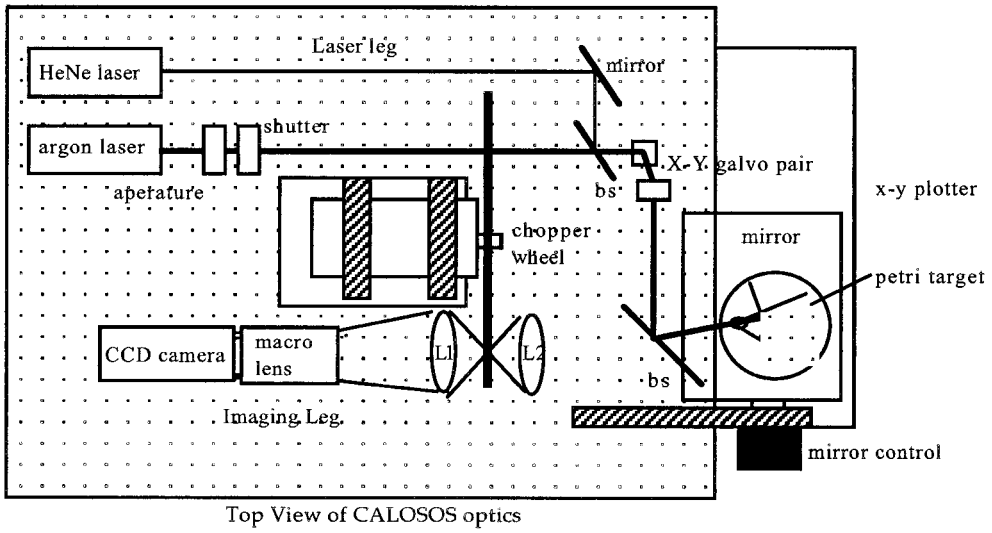

Fig. 7 CALOSOS Optical layout.

it passes through the vanes of the chopper wheel and then magnify the image back to its original size. With this optical configuration, images of the phantom retina may be obtained without the irradiating laser present in the image.

5.3 RETINA CONTROL SOFTWARE

The brain of the CALOSOS system is the RETINA (retinal tracking and image analyzer) software hosted on the 486DX4 100-MHz personal computer discussed earlier. The PC also hosts the associated image processing board (Matrox PIP-1024) and the data acquisition and control board (Data Translation DT2801A). The tracking algorithm is written in "C." Recent software updates provide a user-friendly "Windows-like" interface using the Quinn–Curtis "Real Time Graphics and User Interface Tools" library.

5.4 COMPUTER-CONTROLLED EYE PHANTOM

Prior to testing the CALOSOS system *in vivo* on pigmented rabbits and primate subjects, we wanted to test the system on a retinal phantom target. We chose a petri dish painted with matte black high-temperature paint with a thin layer of egg white. This phantom was previously used in other retinal studies.[4,11,15,33,34] To provide random target movement, the petri dish was attached to the pen carriage of an X-Y plotter (Hewlett Packard 7005B) via an aluminum bracket. Random signals were then provided to the plotter's X and Y inputs via PETRI software hosted on a 386-25 personal computer. The PETRI software is a program written in "C" to generate random numbers at user-specified regular intervals. The random numbers are converted to voltages via a data acquisition and control board (DT2801A) and provided to the X and Y input of the plotter. This configuration allows random petri dish movement at user-specified velocities.

5.5 DATA ACQUISITION SYSTEM

To determine the accuracy of the tracking system, a five-channel data acquisition system has been designed and is hosted on a 486 33-MHz personal computer. A data acquisition board (Data Translation DT2811-PGL) is used to acquire the X and Y random signal driving the retinal phantom target, the X and Y correction signal calculated by the RETINA tracking software, and the shutter control signal. The five channels of data are displayed on a personal computer monitor using the Quinn–Curtis "Real Time Graphics and User Interface Tools." The data are recorded to disk for off-line analysis.

5.6 CALOSOS INTEGRATED SYSTEM PERFORMANCE CONSIDERATIONS AND DESIGN CONCERNS

The CALOSOS integrated system performance requirements fall into three key categories: tracking and compensating for retinal movement, controlling laser pointing and firing, and controlling lesion size. The first two performance requirements fall under the jurisdiction of the previously described lesion placement subsystem. The primary purpose of this subsystem is to place the desired pattern of lesions on the retina without endangering critical vision anatomy. If the patient's eye moves slowly or a small amount, the system will update the required position of the laser. If the eye movement exceeds a threshold, the tracking system must detect it and interrupt the laser firing until the movement subsides and the coordinate system can be reestablished. Thus the primary performance requirements become a specification of eye velocity threshold and response time. With a patient fixating

on a stationary target with the fellow eye, a threshold retinal velocity of 10 degrees/second should allow the system to be used safely with the great majority of patients. Based on 100-ms irradiations, the response time for the tracking algorithm should be 5 ms from the time the eye velocity threshold is exceeded to the time the laser firing is interrupted. This response time is derived from the desire of ophthalmologists to ensure that no more than 1/20 of a typical irradiation elapses before an error condition is corrected (personal communication, H. G. Rylander III). To control laser pointing and firing while forming lesions as small as 200 microns in diameter, a positional accuracy of 100 microns on the retina is required.

The system requirement for controlling lesion size (either diameter or depth) is to provide uniform lesions across the fundus. Thus we have established a performance requirement of achieving consistent lesions within 5% of each other across the lesion pattern, and aborting the lesion if the reflectance versus time parameters exceed some abnormality threshold. Assuming a typical irradiation time of 100 ms implies a sampled resolution of at least 5 ms.

These system requirements have driven the use of a faster system host computer, a faster frame grabber, and investigation of an alternative method of measuring lesion central reflectance. Currently, the host computer is being upgraded to Pentium power while converting to a 32-bit, 40-MHz PCI bus-based frame grabber manufactured by MuTech Corporation. Also, the use of confocal reflectometry to obtain the lesion reflectance data is under investigation.

Several design concerns exist with the CALOSOS integrated system. First, the lesion placement subsystem uses a 50-degree retinal field of view while the lesion depth control subsystem uses a much smaller field of view. Full system testing will indicate if accurate lesion reflectance measurements are possible at the higher field of view. If accurate reflectance measurements are not possible, a dual camera system may be required should the confocal reflectometry efforts yield poor results. Second, some unexpected phenomena were observed while creating laser lesions in an albumen (egg white) eye phantom. Various irradiation times were used for an argon laser (λ = 488, 514 nm) at a power of 475 mW and a spot size of 400 microns. This was a higher power and smaller spot size than used during testing of the lesion depth control subsystem. While lesion diameter increased monotonically with irradiation time in the anticipated fashion, an unexpected effect was observed in the central reflectance of the lesions. For some irradiation times, the central reflectance was actually lower than the edge reflectance, resulting in what visually appeared to be "doughnut-shaped" lesions. This effect has serious implications for a lesion control system that relies upon reflectance.[35] Occasional "doughnut" lesions have been observed in clinical practice (H. G. Rylander III, personal communication) so this is not a phenomenon unique to an eye phantom. The CALOSOS design must take this abnormal occurrence into account and this phenomenon is under detailed investigation.

6 SUMMARY AND CONCLUSIONS

Currently the prototype CALOSOS system is up and operating. However, we are delaying full-up system testing until completion of the computer and frame grabber upgrade described above. Full-up system testing is scheduled to begin in late 1995. From these tests we will answer the design concerns previously discussed. Our goals for the coming year include completing the CALOSOS optical configuration for *in vivo* testing on pigmented rabbit and primate subjects. One of our primary design goals is to make the system independent of a fundus camera and the chopper wheel.

Our research efforts have demonstrated the feasibility of tracking human retinal movement to stabilize an irradiating surgical laser during photocoagulation therapy. A combined dynamic system that is capable of simultaneously creating lesions at specific depths and controlling their placement is required for clinical use. Ongoing and near-term future research activities will put this project in the realm of clinical practicality.

Acknowledgments

This work was supported in part by the Texas Coordinating Board; the Office of Naval Research under grant N00014-91-J-1564; Frank J. Seiler Research Laboratory, USAF Academy, CO; Armstrong Laboratory, Brooks Air Force Base, TX; and Phillips Laboratory, Kirtland Air Force Base, NM. The CALOSOS prototype suite was designed and built as a class project at the USAF Academy in an engineering systems design class taught by Captain Pamela J. Neal. Class students: S. G. Larese (Project Manager), D. J. Abrahamson, M. D. Allen, C. H. Baker, M. T. Bolen, M. Callow, J. Causey, K. E. Devereux, S. H. Drollinger, W. P. Griffiths, C. B. Hudson, A. Mitchell, R. A. Mott, B. M. Patchen, J. L. Plourde, T. D. Rex, and F. Velasco.

REFERENCES

1. M.S. Markow, "The preliminary development of a robotic laser system used for ophthalmic surgery," PhD dissertation, University of Texas at Austin (1987).
2. M.S. Markow, Y. Yang, A.J. Welch, H.G. Rylander III, and W.S. Weinberg, "An automated laser system for eye surgery," *IEEE Eng. in Med. Biol. Mag.*, pp. 24–29 (Dec. 1989).
3. M.S. Markow, H. Grady Rylander III, and A.J. Welch, "Real-time algorithm for retinal tracking," *IEEE Trans. Biomed. Eng.* **40**(12), 1269–1281 (Dec. 1993).
4. M.R. Jerath, C. Gardner, H.G. Rylander III, and A.J. Welch, "Dynamic optical property changes: Implications for reflectance feedback control of photocoagulation," *J. Photochem. Photobio.* **16**, 113–126 (1992).
5. E. Stefansson, R. Machemer, E. de Juan, B.W. McCuen, and J. Peterson, "Retinal oxygenation and laser treatment in pa-

tients with diabetic retinopathy," *Am. J. Ophthalmol.* **113**, 36–38 (Jan. 1992).
6. M.L. Wolbarsht and M.B. Landers, "The rationale of photocoagulation therapy for proliferative diabetic retinopathy: A review and model," *Ophthalmic Surgery* **11**(4), 235–245 (Apr. 1980).
7. G.L. Spaeth, *Ophthalmic Surgery*, pp. 402–408, W.B. Saunders, Philadelphia, PA (1982).
8. M.R. Jerath, R. Chundru, S.F. Barrett, H.G. Rylander III, and A.J. Welch, "Reflectance feedback control of photocoagulation *In Vivo*," *Arch. Ophthalmology* **111**, 531–534 (Apr. 1993).
9. M.R. Jerath, R. Chundru, S.F. Barrett, H.G. Rylander III, and A.J. Welch, "Preliminary results of reflectance feedback control of photocoagulation *In Vivo," IEEE Trans. Biomed. Eng.* **41**(2), 201–203 (Feb. 1994).
10. S.F. Barrett, M.R. Jerath, H.G. Rylander III and A.J. Welch, "Digital tracking and control of retinal images," *Opt. Eng.* **31**, 150–159 (Jan. 1994).
11. M.R. Jerath, "Real time control of laser induced retinal lesions" PhD dissertation, University of Texas at Austin (1992).
12. M.R. Jerath, "A Software package for the analysis of laser induced retinal lesions," Master's thesis, University of Texas at Austin (1989).
13. M.R. Jerath, R. Chundru, S.F. Barrett, H.G. Rylander III, and A.J. Welch, "Reflectance feedback control of photocoagulation *In Vivo," Proc. SPIE* **1877**, 254–261 (1993).
14. S.F. Barrett, M.R. Jerath, H.G. Rylander III, and A.J. Welch, "Automated lesion placement in the rabbit eye," in press, *Lasers in Surgery and Medicine*.
15. S.F. Barrett, M.R. Jerath, H.G. Rylander III, and A.J. Welch, "Instrumentation for feedback controlled retinal photocoagulation," *Proc. SPIE* **1892**, 76–85 (1993).
16. S.F. Barrett, "Digital tracking and control of retinal images," PhD dissertation, University of Texas at Austin (1993).
17. S.F. Barrett, M.R. Jerath, H.G. Rylander III, and A.J. Welch, "Digital tracking and control of retinal images," *Proc. SPIE* **1877**, 272–283 (1993).
18. D.C. West, "Positional control of laser photocoagulator lesions near the fovea," *Brit. J. Ophthalmol.* **52**, 938–939 (1968).
19. G.T. Timberlake, M.A. Mainster, E. Peli, R.A. Augliere, E.A. Essock, and L.E. Arend,"Reading with a macular scotoma- I. Retinal location of scotoma and fixation area," *Invest. Ophand. Vis. Sci.*, **27**, 1137–1139 (1986).
20. D.H. Kelly and H.D. Crane, "Research study of a fundus tracker for experiments in stabilized vision," National Aeronautics and Space Administration, Washington DC (Sept. 1968).
21. H.D. Crane and C.M. Steele, "Accurate three-dimensional eyetracker," *Appl. Opt.* **17**(5), 691–704 (Mar. 1978).
22. D.M. Snodderly, W.P. Leung, G.T. Timberlake, and D.P.B. Smith, "Mapping retinal features in a freely moving eye with precise control of retinal stimulus position," pp 79–91.
23. F. Okuyama and T. Tokoro, "Eye-tracking infra-red optometer," Technical Note.
24. D.I. Barnea and H.F. Silverman, "A class of algorithms for fast digital image registration," *IEEE Trans. Comp.* **C-21**(2), 179–186 (Feb. 1972).
25. E. Peli, R.A. Augliere, and G.T. Timberlake, "Feature-based registration of retinal images," *IEEE Trans. Med. Imaging* **MI-6**(3), 272–278 (Sept. 1987).
26. D. Ott and M. Lades, "Measurement of eye rotations in three dimensions and the retinal stimulus projection using scanning laser ophthalmoscopy," *Ophthal. Physiol. Opt.* **10**, 67–71 (1990).
27. T. Bantel, D. Ott, and M. Rueff, "Global tracking of the ocular fundus pattern imaged by scanning laser ophthalmoscopy," *Int. J. Biomed. Comput.* **27**, 59–69 (1990).
28. J.J. Yu, Y.H. Ho, L. Ko, M. Kao, "Eye-tracking system for computer-assisted photocoagulation," *Ophthalmic Surg.* **22**(5), 260–265 (May 1991).
29. M. Hose, "FFT chips for transform-based image processing," *Advanced Imaging* 56–59 (June 1992).
30. E. De Castro, E. G. Cristini, A. Martelli, C. Morandi, and M. Vascotto, "Compensation of random eye motion in television ophthalmoscopy: Preliminary results," *IEEE Trans. Med. Imaging* **MI-6**(1), 74–81 (Mar. 1987).
31. F.C. Delori, E.S. Evangelos, S. Gragoudas, R. Francisco, and R.C. Pruett, "Monochromatic ophthalmoscopy and fundus photography," *Arch. Ophthalmol.* 861–863 (May 1977).
32. J.B. Zimmerman, S.W. Pizer, E.V. Staab, J.R. Perry, W. McCartney, and B.C. Brenton, "An evaluation of the effectiveness of adaptive histogram equalization for contrast enhancement," *IEEE Trans. Med. Imaging* **7**(4), 304–312 (Dec. 1988).
33. Y. Yang, M.S. Markow, H.G. Rylander III, and A.J. Welch, "Automatic control of lesion size in a simulated model of the eye," *IEEE J. Quantum Electronics* **J-QE**/26, 2232–2239 (1990).
34. M.R. Jerath, D. Kaisig, H.G. Rylander III, and A.J. Welch, "Real time control of lesion size based on reflectance images," *SPIE Proc.* **1644**, 206–216 (1992).
35. C.H.G. Wright, J.K. Barton, H.G. Rylander III, and A.J. Welch, "Reflectance correlation to retinal lesion morphology: Anomalies and ramifications," *Appl. Opt.*, submitted for publication.